



GRB 200826A: A Precursor of a Long Gamma-Ray Burst with Missing Main Emission

Xiangyu Ivy Wang¹ , Bin-Bin Zhang^{1,2} , and Wei-Hua Lei³ ¹ School of Astronomy and Space Science, Nanjing University, Nanjing 210093, People's Republic of China; bbzhang@nju.edu.cn² Key Laboratory of Modern Astronomy and Astrophysics (Nanjing University), Ministry of Education, People's Republic of China³ Department of Astronomy, School of Physics, Huazhong University of Science and Technology, Wuhan 430074, People's Republic of China

Received 2022 February 24; revised 2022 April 23; accepted 2022 May 3; published 2022 May 18

Abstract

The recently discovered peculiar gamma-ray burst GRB 200826A poses a dilemma for the collapsar model. Although all other characteristics of the burst are consistent with it being a Type II (i.e., collapse of a massive star) event, the observed duration of the event is only approximately 1 s, which is at odds with the predicted allowable timescale range for a collapsar event. To resolve this dilemma, this Letter proposes that the original burst could be an intrinsically long GRB comprising a precursor and a main emission phase. However, the main emission phase is missed due to either precession of the jet or the obstruction by a companion star, leaving only the precursor observed as a short-duration GRB 200826A. Interestingly, we found that the temporal and spectral properties of GRB 200826A broadly resembled those of the bright precursor observed in GRB 160625B. Furthermore, assuming the prototype burst of GRB 200826A is similar to that of GRB 160625B, we found that the observer may indeed miss its main emission because of geometric effects caused either by jet precession or companion-obstruction models. Our approach provides a natural explanation for the GRB 200826A-like bursts and agrees with the rarity of those events.

Unified Astronomy Thesaurus concepts: [Gamma-ray bursts \(629\)](#)

1. Introduction

GRB 200826A challenges the traditional observational criteria used to classify short merger-type and long collapsar-type GRBs (Kouveliotou et al. 1993; Zhang et al. 2009). With a short duration of $T_{90} = 0.96_{-0.07}^{+0.06}$ s (Zhang et al. 2021), GRB 200826A distinguishes itself from all other Type I bursts through all of its other observational properties, such as hardness ratio, energy-related correlations, amplitude parameter, spectral lag, and possible supernova association (Ahumada et al. 2021; Rossi et al. 2021; Zhang et al. 2021). Increasing efforts have been made to explain this peculiar GRB. For example, Ahumada et al. (2021) claim that it is the shortest collapsar event, and Zhang et al. (2021) additionally propose several alternatives such as a binary merger invoking a white dwarf (WD) engine, the “supranova” scenario, and a newborn magnetar with a heavy baryon-loading wind. Rather than making any modifications to the GRB’s central engine, we propose in this Letter that GRB 200826A was actually the precursor emission of a long GRB whose main emission (ME) was not observed due to geometric effects.

In terms of geometry, there are two possible configurations that might lead to the absence of GRB emission. One possibility is that the jet slips away, in which case the observer is no longer within the jet cone. Such a slip-away effect can be caused by the precession of the jet. In such a scenario, the jet is powered by a hyperaccreting black hole, and the angular momentum of the black hole is misaligned with respect to that of the accretion disk. The tilted disk is subject to the Lense–Thirring (LT) torque. The LT torque together with the viscosity of the disk causes the inner part of the inclined disk to bend toward the equatorial plane of the black hole, while the outer part of the disk maintains its original orbit (Lense & Thirring 1918; Bardeen & Petterson 1975). The

inner disk would undergo precession. As a result, a precessing disk will induce jet precession (Reynoso et al. 2006; Liu et al. 2010; Lei et al. 2013).

A second possibility is that the jet is completely blocked during the ME, so the observer only observes the precursor. This may occur if the GRB is in a binary system (Zou et al. 2021). Such a system is composed of a GRB central engine and a stellar companion. If the observer is on axis and the companion star is located within the jet-opening angle⁴ (case I in Zou et al. 2021), the observed GRB properties are determined by the observation angle (the angle between the jet direction and the observer’s line of sight), the Lorentz factor of the jet, and the obstruction by the companion star. If the observer is on axis and the Lorentz factor is greater than a critical value, the companion star can block the GRB emission so that the on-axis observer completely misses it. For GRB 200826A, we demonstrate in this Letter that the ME can be entirely blocked by using an appropriate Lorentz factor value and geometric configuration.

This Letter starts by comparing the observed properties of GRB 200826A with the precursor of the typical three-episode GRB 160625B, aiming to find observational evidence of their similarities (Section 2). The jet-precession (Section 3.1) and companion-obstruction (Section 3.2) models are then applied to explain the observations of GRB 200826A as well as its possibly missing ME. A brief conclusion and discussion are presented in Section 4.

2. GRB 200826A as a Precursor

GRB 200826A is considered a precursor of a long GRB due to the following facts:

1. Temporal and spectral properties consistent with the precursors of other GRBs. GRB precursors are always

Original content from this work may be used under the terms of the [Creative Commons Attribution 4.0 licence](#). Any further distribution of this work must maintain attribution to the author(s) and the title of the work, journal citation and DOI.

⁴ Here we consider a top-hat jet with $\theta_j \gg 1/\Gamma$ during the prompt-emission phase of the GRB, where Γ is the Lorentz factor of the ejecta. In this case, only a small fraction of the emitting surface of the jet is observable. This region is centered on the line of sight and has an opening angle of $1/\Gamma$.

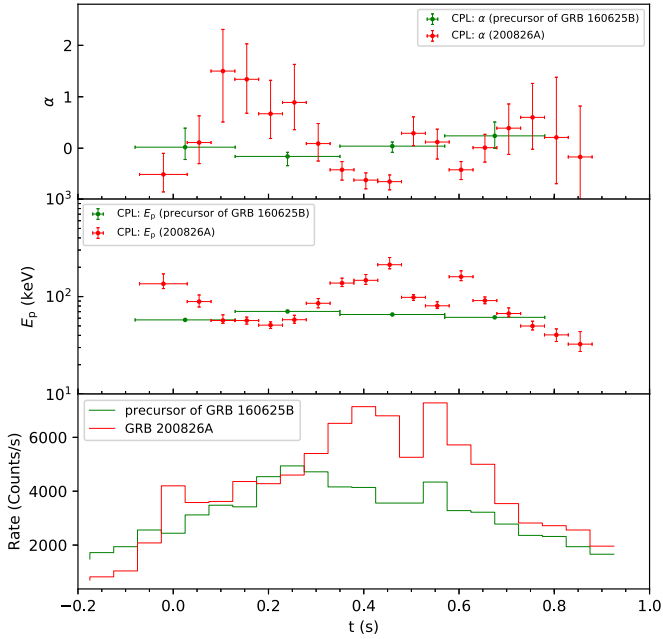


Figure 1. Comparison of the spectral evolution between GRB 200826A and the precursor of GRB 160625B. Both bursts are fitted by the cutoff power law (CPL) model. The bottom panel shows the comparison of the light curves of the two events. Data are taken from Zhang et al. (2018) and Zhang et al. (2021).

characterized by a short duration and thermal emission (Li 2007). Indeed, the duration of GRB 200826A is only 1 s, similar to the typical duration of precursors in long GRBs (e.g., GRB 160625B; Zhang et al. 2018). Moreover, the spectral evolution of GRB 200826A (Figure 1) shows that its low-energy indexes, α , are greater than zero in about two-thirds of the time slices, which are consistent with a thermal origin.

2. Location on the $E_p - E_{\text{iso}}$ diagram consistent with those of the precursors in other GRBs. The burst is located at the long (Type II) GRB track on the $E_p - E_{\text{iso}}$ diagram, which is similar to the precursors of other long GRBs. As an example, we plot both GRB 200826A and the precursor of GRB 160625B, a typical three-episode-long GRB with significant precursor emission, on the $E_p - E_{\text{iso}}$ diagram in Figure 2. One can see that the two events both reside on the Type II GRB track.
3. Almost identical to the precursor of GRB 160625B. In Table 1 and Figure 1, we compare the temporal and spectral properties between GRB 200826A and the precursor phase of GRB 160625B. The two events display striking similarities in the following aspects: (1) similar duration. Both of their T_{90} values are roughly equal to 1 s. (2) Similarly strong signal-to-noise ratios. As shown in Table 1, the f-parameter values, which measure the “tip-of-the-iceberg” effect of a GRB (Lü et al. 2014), of the two GRBs are both above 3, indicating strong signals above the background (Figure 3). (3) Similar temporal and spectral evolution patterns. As shown in Figure 1, the light curves of both events are single-pulse shaped. Although GRB 200826A has a stronger spectral evolution, its spectral parameters (such as the low-energy index, α , and spectral peak energy, E_p) are overall in a range consistent with those of the precursor of GRB

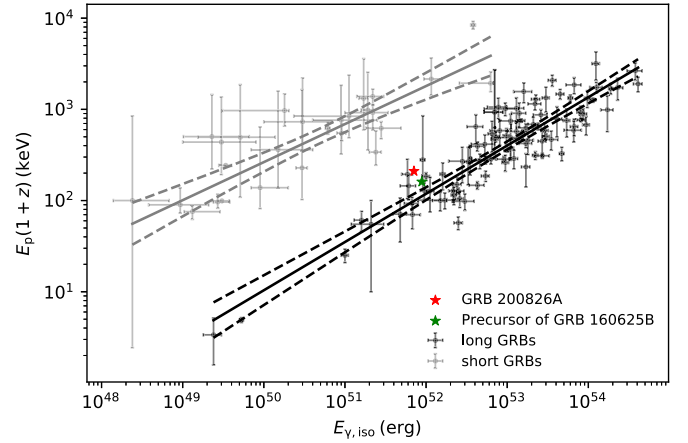


Figure 2. The $E_{p,z}$ vs. $E_{\gamma,\text{iso}}$ correlation diagram. The black and gray solid lines are the best linear correlations for long and short GRBs, respectively. GRB 200826A (red star) and the precursor of GRB 160625B (green star) both fall in the long-GRB region. The samples are from Amati et al. 2002 and Zhang et al. (2009).

Table 1

Properties of GRB 200826A and the Precursor of GRB 160625B (Zhang et al. 2021, 2018)

	GRB 200826A	Precursor of GRB 160625B
z	0.7481	1.406
T_{90} (s)	$0.96^{+0.06}_{-0.07}$	$0.84^{+0.03}_{-0.01}$
f-parameter	7.58 ± 1.23	3.42 ± 0.14
Peak energy (keV)	$120.29^{+3.93}_{-3.67}$	$66.8^{+1.8}_{-1.8}$
Peak flux (10^{-6} erg cm^{-2} s^{-1})	$9.11^{+1.47}_{-1.17}$	$2.42^{+0.11}_{-0.11}$
Fluence (10^{-6} erg cm^{-2})	4.85 ± 0.19	1.75 ± 0.05
Isotropic energy (10^{51} erg)	7.09 ± 0.28	8.86 ± 0.24

160625B. Both events exhibit strong thermal-like spectral features in $>80\%$ time slices.

In summary, GRB 200826A is fully consistent with being a precursor of a long-GRB event. The question is how the ME of such a long GRB can be missed by an observer.

3. How Can We Miss the Main Emission?

To miss the ME, either the jet had to slip away within a certain time frame or the jet had to be blocked during the ME. The two scenarios correspond to the following two different physical pictures.

3.1. Jet Precession

Jet precession has long been proposed (e.g., see Liu et al. 2010) for GRBs whose central engine consists of a rapidly hyperaccreting black hole. For a long GRB, the anisotropic explosions of its progenitor star lead to the misalignment between the disk and angular momentum of the black hole. In such a scenario, the Bardeen–Pettersson (BP) effect (Bardeen & Pettersson 1975) tends to align the inner part of the inclined disk with the equator of the black hole while the outer part of the disk maintains its original orbit. The outer disk will lead to the precession of the inner disk and the black hole (Sarazin et al. 1980; Liu et al. 2010; Sun et al. 2012) due to the LT effect,

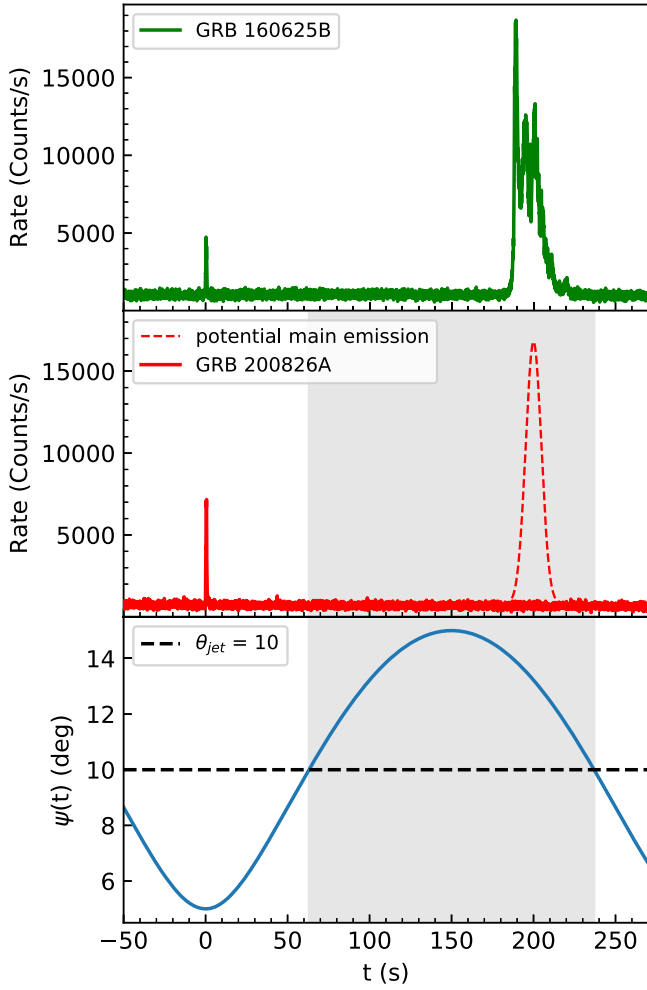


Figure 3. Top: light curve of GRB 160625B. Middle: The solid red line is the light curve of GRB 200826A. The dashed red line is the assumed ME of the prototype burst. Bottom: The solid blue line shows how the viewing angle $\psi(t)$ changes over time, and the dashed black line is the jet-opening angle. The gray shaded area is where the ME can be missed by the observer.

which is known as disk-driven precession. The jet will precess because its direction is determined by the spin axis of the black hole, and its precession period is the same as the LT precession period.

The jet precession model has been utilized to interpret various shapes of GRB light curves (e.g., Portegies Zwart et al. 1999; Lei et al. 2007) and their complex temporal and spectral evolution (Liu et al. 2010). There is a possibility that, in some cases, the ME might be missed as a result of jet precession. Here we will show that GRB 200826A may be such a case.

As schematized in Figure 4, we assume the jet is conical and no moving material is outside the cone. Salafia et al. (2016) studied the effect of viewing angle $\psi(t)$ on GRB peak flux and showed that the peak flux can be written as a function of $\psi(t)$:

$$F_p(\psi(t))/F_p(0) = \begin{cases} 1, & \theta_{\text{jet}} \geq \theta_{\text{jet}}^*, \\ \frac{1 - \Gamma(\psi(t) - \theta_{\text{jet}})}{2}, & \theta_{\text{jet}}^* < \psi(t) \leq \theta_{\text{jet}}, \\ \frac{1}{2} \left(\frac{D}{(1 + \beta)\Gamma} \right)^{(4 - \sqrt{2}\theta_{\text{jet}}^{1/3})}, & \psi(t) > \theta_{\text{jet}}, \end{cases} \quad (1)$$

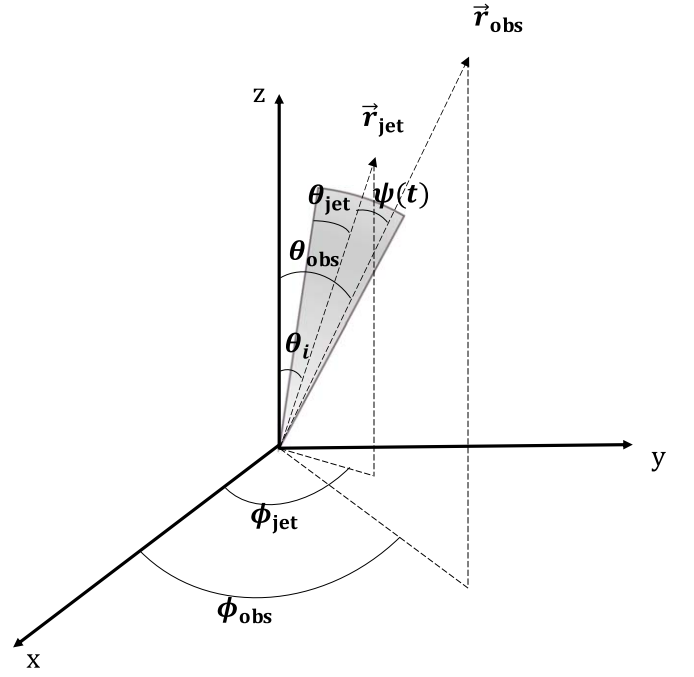


Figure 4. The schematic sketch of the precession jet model.

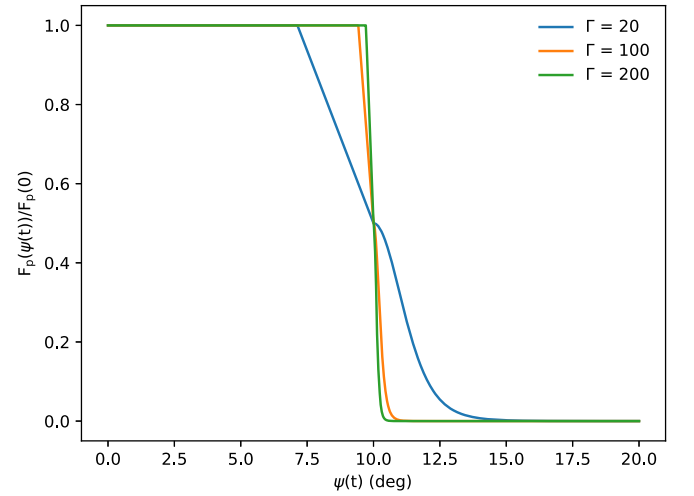


Figure 5. The blue, orange, and green lines represent the evolution of the observed peak flux with the viewing angle when the Lorentz factor $\Gamma = 20$, 100, and 200, respectively.

where $\theta_{\text{jet}}^* = \theta_{\text{jet}} - \frac{1}{\Gamma}$, $\beta = \sqrt{1 - \Gamma^{-2}}$, $F_p(0)$ is the observed peak flux when the line of sight is centered on the jet axis, and D is the Doppler factor defined as $D = \frac{1}{\Gamma(1 - \beta \cos \psi(t))}$.

Figure 5 shows the observed peak flux changes over the viewing angle $\psi(t)$ with $\theta_{\text{jet}} = 10^\circ$. One can see that the larger the Lorentz factor, the sharper the peak flux drops as the line of sight in the direction of \mathbf{r}_{obs} moves away from θ_{jet}^* . For a jet with a Lorentz factor of $\Gamma > 200$ (e.g., $\Gamma \geq 214$ for the precursor of GRB 160625B; Zhang et al. 2018), we can assume that no flux would be received by the observer once $\psi(t)$ exceeds θ_{jet} , and the observed flux can be written as a function of $\psi(t)$:

$$F(\psi(t)) = \begin{cases} F(0), & \theta_{\text{jet}} > \psi(t), \\ 0, & \theta_{\text{jet}} < \psi(t). \end{cases} \quad (2)$$

Following Hou et al. (2014a, 2014b), the precession period can be expressed as

$$\tau = 2793a_* \left(\frac{M_{\text{BH}}}{M_\odot} \right)^{\frac{7}{13}} \left(\frac{\dot{M}}{M_\odot \text{s}^{-1}} \right)^{-\frac{30}{13}} \alpha^{\frac{36}{13}} \text{s}, \quad (3)$$

where a_* is the spin parameter, M_{BH} is the mass of the rotating black hole, \dot{M} is the accretion rate in units of $M_\odot \text{s}^{-1}$, and α is the viscosity parameter of the accreting disk. In the rest frame of the observer, the precession period is $\tau' = (1+z)\tau$. For a standard collapsar model (MacFadyen & Woosley 1999), the $14M_\odot$ helium core of a $35M_\odot$ main-sequence star would collapse to form a 2 to $\sim 3M_\odot$ black hole. Inserting $a_* = 0.9$, $M_{\text{BH}} = 3M_\odot$, $\dot{M} = 0.1M_\odot \text{s}^{-1}$, and $\alpha = [0.01, 0.1]$ into Equation (3), we get $\tau' = [4.52, 2655.67] \text{ s}$. Here, we take $\tau' = 300 \text{ s}$ in the following analysis.

For a conical jet, the angle $\psi(t)$ between the observer and the jet axis can be written as

$$\cos(\psi(t)) = \cos \theta_{\text{obs}} \cos \theta_i + \sin \theta_{\text{obs}} \sin \theta_i \cos \beta, \quad (4)$$

where $\beta = \frac{2\pi}{\tau}t + \beta_0$, and $\beta_0 = \phi_{\text{obs}} - \phi_{\text{jet}}$. Taking $\theta_{\text{obs}} = 10^\circ$, $\theta_i = 5^\circ$, $\beta_0 = 0$, and $\theta_{\text{jet}} = 10^\circ$, the observational angle $\psi(t)$ as a function of time is plotted in the lower panel of Figure 3. According to Equation (2), when $\psi(t)$ is larger than the jet-opening angle (the black dashed line), the GRB flux will be missed by the observer. The gray shaded area in Figure 3 marks the time range during which the GRB emission can be missed. Using the assumption that the prototype GRB 200826A is a GRB 160625B-like event that has an ME of 40 s duration around $t = 200 \text{ s}$, one can find that the ME can be completely missed due to the precession effect.

3.2. Companion Star Obstruction

If a GRB is accompanied by a stellar companion with a radius of R_c , which happens to be located inside the jet-opening angle, the GRB emission with a radius of R_{GRB} can be partially or fully blocked (Zou et al. 2021). In such a scenario, the absence of the ME can be explained by the full obstruction by the companion star, as illustrated in Figure 6. First, the precursor is not blocked before the companion star enters within a certain solid angle (calculated below) along the line of sight, allowing the observer to receive the precursor emission as usual (Figure 6(a)). Then, due to the orbital motion, if the companion star moves into the line of sight and meets the requirements for a full-obstruction condition, the observer can entirely miss the ME (Figure 6(b)). Assuming the radiation is from the radially relativistically expanding surface, the radiation of each point of the emission surface will beam into a conical angle of radius $1/\Gamma$ in the direction of its velocity. Consequently, the observer will only receive photons within the $1/\Gamma$ cone of a conical jet along the line of sight (between A and B in Figure 6). We assume a typical top-hat jet with an opening angle of $\theta_{\text{jet}} \sim$ a few degrees, much larger than the beaming angle of $1/\Gamma$ as the Lorentz factor may reach several hundred during the prompt-emission phase. The full-obstruction condition can be expressed numerically as follows:

1. The observer can only receive the photons within the θ_0 cone. θ_0 is defined as $\theta_0 = \frac{1}{\Gamma}$, with Γ being the Lorentz factor of the ejecta. The maximal obstruction angle by the companion star (i.e., the opening angle of the blocked

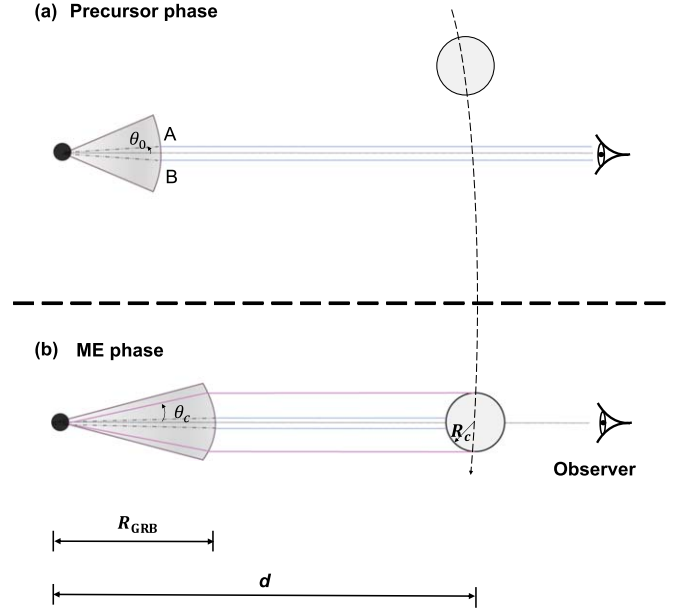


Figure 6. The schematic sketch of the companion-obstruction model. See also Zou et al. (2021). (a) The configuration of the system during the precursor phase. (b) The configuration for the ME phase.

emission surface with respect to the GRB central engine; Zou et al. 2021), $\theta_c = \frac{R_c}{R_{\text{GRB}}}$, must exceed the maximal observed cone angle θ_0 .

2. During the time gap between the precursor and ME, the motion angle of the companion star must exceed $2\theta_0$ in order to occult the ME.
3. During the ME phase, the motion angle of the companion star could not exceed $2\theta_c - 2\theta_0$. Otherwise, the observer would receive the flux of the ME at its late stage.

These conditions can be written as

$$\theta_c \geq \theta_0; \quad (5a)$$

$$\Omega t_w \geq 2\theta_0; \quad (5b)$$

$$\Omega t_m \leq 2\theta_c - 2\theta_0, \quad (5c)$$

where $\Omega = \sqrt{\frac{GM_{\text{total}}}{d^3}}$ is the angular velocity of the companion star, M_{total} is the total mass, d is the distance between the central engine and the stellar companion, t_m is the duration of the ME, and t_w is the waiting time between the precursor and the ME. In our analysis, $t_m = 35 \text{ s}$ and $t_w = 180 \text{ s}$ (Zhang et al. 2018) are adapted in accordance with the those of GRB 160625B.

Assuming a typical parameter set with $M_{\text{total}} = 50M_\odot$, $\Gamma = 800$, $R_{\text{GRB}} = 10^{11} \text{ cm}$, (i.e., a typical photosphere radius; however, see Zhang et al. 2018), and $R_c = 0.02R_\odot$ ($1.39 \times 10^9 \text{ cm}$), d can be constrained at $d \leq 3.25 \times 10^{12} \text{ cm}$ according to Equation (5b).

4. Summary and Discussions


In this paper, we suggested that the Type II short GRB 200826A may actually be a precursor of a long GRB whose main emission was missed by the observer. The absence of the main emission is further explained by geometrical models that invoke either the precession of the jet or obstruction by the companion star. By assuming that GRB 160625B serves as a prototype of GRB 200826A, we were able to successfully

apply these two models and reproduce the GRB 200826A event by omitting the ME of the prototype burst. Even though both models provide acceptable fits, the companion-obstruction model requires more fine-tuning of the parameters and even coincidental alignment between the GRB and the companion star, which, on the other hand, is in agreement with the rarity of the event. Nevertheless, our results shed some alternative light on how to explain the GRB 200826A-like events. Future observations of similar events will be helpful to test the hypothesis proposed in this paper.

We thank Z.-C. Zou and X.-H. Zhao for helpful discussions on the paper. B.B.Z. acknowledges support by the National Key Research and Development Programs of China (2018YFA0404204), the National Natural Science Foundation of China (grant Nos. 11833003, U2038105, 12121003, U2038107, and U1931203), the science research grants from the China Manned Space Project with No. CMS-CSST-2021-B11, and the Program for Innovative Talents, Entrepreneur in Jiangsu. We acknowledge the use of public data from the Fermi Science Support Center (FSSC).

ORCID iDs

Xiangyu Ivy Wang  <https://orcid.org/0000-0002-9738-1238>

Bin-Bin Zhang  <https://orcid.org/0000-0003-4111-5958>

Wei-Hua Lei  <https://orcid.org/0000-0003-3440-1526>

References

- Ahumada, T., Singer, L. P., Anand, S., et al. 2021, *NatAs*, **5**, 917
 Amati, L., Frontera, F., Tavani, M., et al. 2002, *A&A*, **390**, 81
 Bardeen, J. M., & Petterson, J. A. 1975, *ApJL*, **195**, L65
 Hou, S.-J., Gao, H., Liu, T., et al. 2014b, *MNRAS*, **441**, 2375
 Hou, S.-J., Liu, T., Gu, W.-M., et al. 2014a, *ApJL*, **781**, L19
 Kouveliotou, C., Meegan, C. A., Fishman, G. J., et al. 1993, *ApJL*, **413**, L101
 Lei, W. H., Wang, D. X., Gong, B. P., & Huang, C. Y. 2007, *A&A*, **468**, 563
 Lei, W.-H., Zhang, B., & Gao, H. 2013, *ApJ*, **762**, 98
 Lense, J., & Thirring, H. 1918, *PhyZ*, **19**, 156
 Li, L.-X. 2007, *MNRAS*, **380**, 621
 Liu, T., Liang, E. W., Gu, W. M., et al. 2010, *A&A*, **516**, A16
 Lü, H.-J., Zhang, B., Liang, E.-W., Zhang, B.-B., & Sakamoto, T. 2014, *MNRAS*, **442**, 1922
 MacFadyen, A. I., & Woosley, S. E. 1999, *ApJ*, **524**, 262
 Portegies Zwart, S. F., Lee, C.-H., & Lee, H. K. 1999, *ApJ*, **520**, 666
 Reynoso, M. M., Romero, G. E., & Sampayo, O. A. 2006, *A&A*, **454**, 11
 Rossi, A., Rothberg, B., Palazzi, E., et al. 2021, arXiv:2105.03829
 Salafia, O. S., Ghisellini, G., Pescalli, A., Ghirlanda, G., & Nappo, F. 2016, *MNRAS*, **461**, 3607
 Sarazin, C. L., Begelman, M. C., & Hatchett, S. P. 1980, *ApJL*, **238**, L129
 Sun, M.-Y., Liu, T., Gu, W.-M., & Lu, J.-F. 2012, *ApJ*, **752**, 31
 Zhang, B., Zhang, B.-B., Virgili, F. J., et al. 2009, *ApJ*, **703**, 1696
 Zhang, B. B., Liu, Z. K., Peng, Z. K., et al. 2021, *NatAs*, **5**, 911
 Zhang, B. B., Zhang, B., Castro-Tirado, A. J., et al. 2018, *NatAs*, **2**, 69
 Zou, Z.-C., Zhang, B.-B., Huang, Y.-F., & Zhao, X.-H. 2021, *ApJ*, **921**, 2